

Effects of Silica Modified NiFe₂O₄ on the Dielectric and Electrical Properties of NiFe₂O₄ filled Poly (methyl methacrylate) Composites

Srikanta Moharana^{1,3}, Anjali Kujur², Sudhir Minz², R. N. Mahaling³, Banarji Behera^{2,*}

^{1,3}Materials Research Laboratory, School of Applied Sciences, Centurion University of Technology and Management, Odisha, India

²Materials Research Laboratory, School of Physics, Sambalpur University, Jyotivihar, Burla, Odisha, India

³Laboratory of Polymeric and Materials Chemistry, School of Chemistry, Sambalpur University, Jyotivihar, Burla, Odisha, India

*Corresponding author: E-mail: banarjibehera@gmail.com, rnmahaling@suniv.ac.in; Tel: (+91) 663-2431 719

DOI: 10.5185/amlett.2020.021480

Nickel ferrite [NiFe₂O₄ (NFO)] nanoparticles were synthesized using a simple precursor based chemical route and modified with tetraethoxysilane (TEOS) to form SiO₂ layer adsorbed on the NFO particles (SiO₂@NFO). Based on the nanoparticles, the SiO₂@NFO-PMMA composite films were prepared embedded with SiO₂@NFO nanoparticles in a poly (methylmethacrylate) (PMMA) matrix. The properties of the composites were characterized extensively using X-ray diffraction (XRD), scanning electron microscopy (SEM), Fourier transform infrared (FTIR) spectroscopy, dielectric and electrical measurement. FTIR analysis showed that the SiO₂ groups had been successfully introduced into the NFO nanoparticles. The SEM images of the SiO₂ adsorbed NFO nanoparticles had better dispersion in the PMMA matrix than the unmodified one. The SiO₂ modified NFO-PMMA composites had much higher dielectric constant and better suppressed dielectric loss than the other two phase composite systems. The maximum dielectric constant was up to ≈ 67 while the dielectric loss was controlled below 0.5. This study suggested that the SiO₂ modified NFO-PMMA composite films with high dielectric constant and low loss might be promising candidates for application in microelectronic engineering.

Introduction

Recently, considerable research interest is emphasized on the investigations of ferrite-polymer composite materials among researchers and industries. This is because the polymers are flexible, easy of processing, minimum cost and different applications [1-3]. While the combination of polymer and spinel ferrites may give the composites some benefits i.e., the progress of new composite materials that have excellent dielectric and electrical properties is still challenging [4-6].

In particular, Nickel ferrite (NiFe₂O₄; NFO) is one of the most versatile spinel ferrites and ferromagnetic in nature. This originates from anti-parallel spins between Ni²⁺ and Fe³⁺ ions at octahedral and tetrahedral sites, respectively [7]. These materials have unique properties such as good dielectric constant, low loss, low conductivity, high electrical resistivity and considerable thermal and chemical stability [8-9]. However, the NiFe₂O₄ nanoparticles have mixed spinel structure, where tetrahedral sites may be occupied by Ni²⁺ ions. The materials also exhibit super-paramagnetic nature and have widely applied in the manufacture of electronic devices including magnetic gas sensors, recording media,

microwave devices, lithium ion batteries, hydrogen production, telecommunication industries [10-13]. Polymers such as poly(methylmethacrylate) (PMMA) is an important transparent thermoplastic material exhibiting moderate physical properties, high dielectric strength, easy processing, low cost and good stability [14]. Generally, the common polymers have very low dielectric constant (<10). The multifunctional composite materials consisting of magnetic nanoparticles including cobalt ferrite (CoFe₂O₄) [15], nickel ferrite (NiFe₂O₄) [16] and iron oxide (Fe₃O₄) [17] dispersed in a polymer matrix have been studied due to excellent dielectric and electrical properties for wide spread technological applications [15-20]. The ferrite based polymer composite films with flexible, light weight and ability to easily control in various shapes along with performance and properties of nanoparticles fulfil the requirement of specific engineering applications [19-20]. Besides, the useful characteristic of polymer matrix is the chance of mediating magnetic interaction between the particles in the composites with dipolar, ex-change (isotropic & anisotropic), super exchange and magneto elastic interactions [20-21]. There are many researchers those have studied nickel ferrite containing various cations, but few have reported based on

nickel ferrite-polymer composites. The polymer composites with very high volume fraction of nickel ferrite (>50 vol%), which may affect the mechanical, dielectric and electrical properties [22-23]. However, owing to the difference of surface energy between inorganic filler particles and polymer matrix, agglomerations in the composites have a crucial effect on the dielectric and electrical behavior. For minimizing agglomeration, a few types of surface modifying agents are used for uniform dispersion of ferrite particles into the polymer matrix [24]. So far, many techniques have been made to solve these problems and enhance the dielectric and electrical properties of the composites [25-29]. Thus, the appropriate surface modifying agent is necessary to fabricate ferrite based polymer composites for better energy storage properties. Meanwhile, the incorporation of the nanoparticles produce a large number of interfaces in the polymer and these interfaces influence the dielectric properties of the composite materials by store and transport charge [30]. A variety of studies to date have employed that the addition of nanoparticles can improve the electrical properties of the polymer [30-33]. In magnetic nanoparticle-polymer composite systems, Mariatti *et al.* [18] have prepared the effect of Ni-Zn ferrite-epoxy composite films with improved dielectric properties. In these composite systems, the value of dielectric constant (ϵ_r) and dielectric loss ($\tan \delta$) increases with the variation of filler content because of interfacial and dipolar polarization. He *et al.* [31] have studied graphene nanosheets (GNS)-Fe₃O₄-syndiotactic polystyrene composite films with enhanced dielectric and electrical performance in the field of high charge storage capacitor applications. Piyushch *et al.* [32] have fabricated dielectric properties of carbon coated nickel nanoparticle-poly (dimethylsiloxane) (PDMS) composites in various frequency ranges and is seen that the value of ϵ_r increases linearly with the increase in the filler content. Similarly, Mendez *et al.* [33] have also examined the dielectric and magnetic properties of poly (vinylidene fluoride) (PVDF) based nanocomposites using cobalt or nickel ferrites via solvent casting techniques. The effect of dielectric constant on these nanocomposites increases with increase in the ferrite content but the cobalt ferrite composites have high value of ϵ_r than the nickel ferrite owing to the polar nature of polymeric phase at low concentration.

In the present work, the SiO₂ modified NiFe₂O₄ (SiO₂-NiFe₂O₄) nano dielectric PMMA composites are synthesized *via* solution casting technique. Here, SiO₂ groups are chosen as the shell layer due to its good properties and adsorbed on the ferrite nanoparticles and polymer matrix. The resultant composite shows significant increase of ϵ_r and relatively lower $\tan \delta$ than that of the non-modified NiFe₂O₄-polymer composites. The high value of ϵ_r is achieved \approx 67 at 100 Hz, while the dielectric loss is suppressed below 0.5. These experimental results provide a valuable approach to fabricate uniform ferrite-polymer composites and facilitate their uses in the embedded capacitors and other energy storage devices.

Experimental

Materials

The chemicals Ni (NO₃)₂.6H₂O, Fe (NO₃)₃.9H₂O, Ethylene di-amine tetra acetic acid (EDTA; 99.9%, Merck, India), Tetraethoxysilane (TEOS) was obtained from Sigma Aldrich, India. Poly (methylmethacrylate) (PMMA) from M/sHimedia Pvt. Ltd., India was used to preparing the composites. The solvent of N, N-dimethylformamide (DMF) was purchased from Spectrochem Pvt. Ltd., Mumbai, India. All the materials were of analytical grade and used with no further purification. Double distilled water was used over the whole experiment.

Synthesis of Nickel Ferrite (NFO) Nanoparticles

NiFe₂O₄ (NFO) nano-particles were prepared *via* EDTA Precursor based chemical route. Briefly, the stoichiometric amount of Nickel Nitrate and Ferric Nitrate were prepared by dissolved in distilled water with a molar ratio of 1:2. These two solutions were mixed in a beaker. On the other hand, an aqueous solution (EDTA) was prepared by dissolving EDTA in hot water with drop wise addition of dilute NH₄OH solution. After total dissolution of EDTA, the solution was boiled to taken out the excess NH₃. The pH of the solution was found to be 6. To this solution, the aqueous solution of the metal nitrate and EDTA were mixed in a molar ratio of 1:1 and continuously stirred for 1h at room temperature. Finally, the pH of the resulting mixture was 2. Then this solution was evaporated to dryness using a hot plate at 110° C. Towards the end of the reaction, a black colour precursor was obtained at the base of the beaker. Then the product was calcined at 900°C for 2 hours and form Nickel ferrite Nano-particle. The preparation of nickel ferrite nano-particle is shown in the flow chart (Fig. 1).

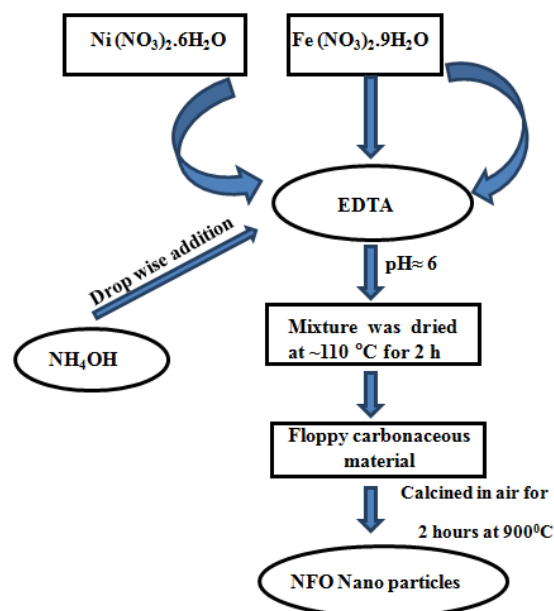


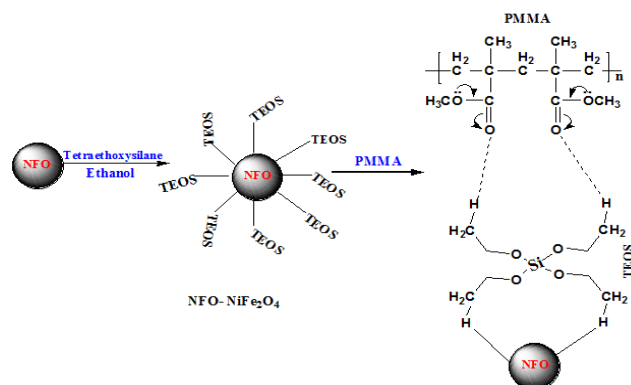
Fig. 1. Flow chart of preparation of NiFe₂O₄ nanoparticles.

Preparation of the SiO₂@NFO nano-particles

The SiO₂@NFO nanoparticles were synthesized using the sol-gel technique. In the process of surface modification, the stoichiometric amount of Nickel Nitrate and Ferric Nitrate were dissolved in ethanol according to their molar ratio of 1:2. Further, an aqueous solution of EDTA was prepared by dissolving EDTA in hot water with the drop wise addition of dilute NH₄OH solution and TEOS (70 wt %) was added into the solution. Then, these two solutions were mixed homogeneously under stirring at room temperature. Ammonia was added drop-wise in the mixture to adjust the pH value to 6. Then the temperature was increased up to 70°C and by continuous stirring a gel was formed. After, the formation of the gel, the sample was dried at 70°C for 24h and then at 110°C under vacuum for 5h. Finally, the product was calcined at 900°C for 2h to obtain modified nickel ferrite nanoparticles.

Fabrication of the SiO₂@NFO-PMMA composite films

The composites of SiO₂@NFO-PMMA were prepared through a simple solution casting technique. In this technique, firstly, PMMA (pallet) was dissolved in N, N-dimethylformamide (DMF) with constant stirring for 30 minutes at 90°C and obtained a clear solution. Secondly, the modified NFO nanoparticles were dispersed into the DMF. Then the mixtures were added into the PMMA solution under constant stirring for 1h and further, ultrasonication for 30 minutes in order to know the uniform dispersion of NFO nanoparticles. The output suspension was cast into a glass (clean) petridish and placed in a vacuum oven to evaporate the solvent. Then the products, NFO-PMMA composite films were obtained. This composite film was then subjected for the various physiological characterizations. The plausible mechanism for the fabrication of tetraethoxysilane modified nickel ferrite-PMMA nano-dielectric composites is shown in the Scheme-1.



Scheme 1. Reaction scheme for the preparation process of SiO₂ modified NiFe₂O₄-PMMA composite.

Characterization techniques

The crystal structure of the pure NFO, SiO₂ modified NFO nanoparticles and composite films were characterized by X-ray diffraction (XRD; Ultimate IV, Rigaku Japan) with Cu K_α radiation where λ = 1.5405 Å (at room temperature).

The diffraction data (2θ) were collected over the scanning range of 10-80° with a step size of 0.02°. Fourier transform infrared spectrometry (FT-IR) of unmodified and modified samples were recorded using a Nicolet 5700 spectrometer in the range of 400-4000 cm⁻¹ to determine the functionalization of the NFO nanoparticles. The morphology of the prepared composite films was carried out via scanning electron microscope (SEM, ZEISS EVO-18). The dielectric and electrical properties of the films were measured by using an impedance analyser (HIOKI, Japan; IM 3570) in the frequency range of 100 Hz to 1 MHz at room temperature.

Results and discussion

The synthetic strategy used for the preparation of NFO-PMMA and SiO₂@NFO-PMMA composite films in this investigation is schematically illustrated in Scheme 1. Firstly, the NiFe₂O₄ nanoparticles were prepared by a precursor based chemical route. Then the SiO₂ modified NFO nanoparticles were synthesized via a sol-gel process using tetraethoxysilane as a precursor. The SiO₂@NFO-PMMA composite films were prepared using solution casting technique. As the schematic pictures shown in Scheme 1, quantities of silica layers were attached to the NFO surface by using sol-gel technique. When the modified nanoparticles were mixed with PMMA, hydrogen bond will form between the O atoms on the PMMA and the H atoms on the surface of the SiO₂ modified NFO nanoparticles. Because of this, a strong interaction between SiO₂ modified NFO nanoparticles and PMMA matrix were produced.

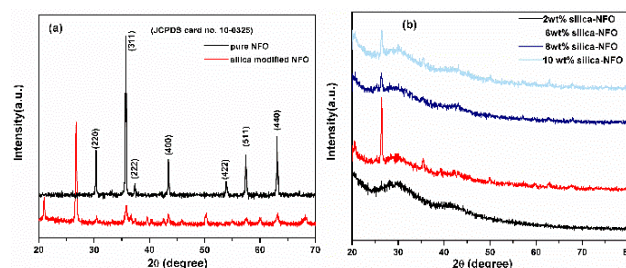


Fig. 2. X-ray diffraction patterns of (a) pure nickel ferrite (NiFe₂O₄: NFO), silica modified NFO and (b) different weight percentage of silica modified NFO-PMMA composite films.

X-ray diffraction analysis

X-ray diffraction (XRD) patterns (Fig. 2) of the (a) pure NFO, SiO₂ modified NFO and (b) different weight percentage of silica modified NFO-PMMA composite films. As it can be seen, pure nickel ferrite (Fig. 1 (a)) shows Bragg reflections which are clearly identified as the formation of face centered cubic (fcc) and pure inverse spinel structure of single phase with Fd3m space group is confirmed by matching with JCPDS card no: 10-0325 [34-35]. The appearance of a characteristic peaks at 2θ ≈ 30.3°, 35.8°, 37.3°, 43.3°, 53.9°, 57.3° and 63.1° refers to crystal planes of (220), (311), (222), (400), (422), (511) and (440), respectively. For the silica modified NFO

nanoparticles, the extra peak at around 22° to 26° , the left shift of peaks correspond to the amorphous SiO_2 adsorbed on the NFO nanoparticles [36-37]. Fig. 2(b) shows SiO_2 modified NFO-PMMA films (composite) as a function of various weight percentages of modified NFO nanoparticles was obtained by XRD. From these patterns, it is clearly noticed that the appearance of sharp peaks at $2\theta \approx 26^\circ$ corresponding to the amorphous phase of SiO_2 groups, while the characteristic peaks near $2\theta \approx 30^\circ$ may be due to the presence of amorphous polymer chain. Moreover, it can be observed that with the increase in percentage of SiO_2 modified NFO nanoparticles in the polymer matrix, the intensity and sharpness of the peaks were disappeared, which indicates the increase of the amorphous nature of the composites. These pattern exhibits typical amorphous nature of the composite material. Further, it is noted that similar results have been reported in the earlier literature for PMMA [38-39].

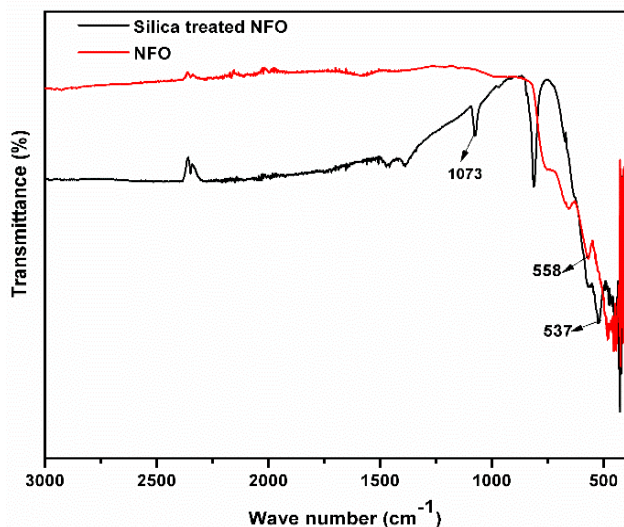


Fig. 3. FTIR spectra of silica modified NFO nanoparticles.

FT-IR analysis

Fig. 3 shows the FTIR spectra of the pure NFO and SiO_2 modified NFO nano-powders. The characteristic absorption band in the region of 1073 cm^{-1} is attributed to the stretching vibration of Si-O-Si group which signifies that the silica groups were successfully modified on the NFO nanoparticles. Further, the characteristic absorption band at 537 and 558 cm^{-1} corresponds to bond between Fe-O stretching and bending vibration of NFO nanoparticles [40].

Surface morphology

The microscopic images of NFO-PMMA and SiO_2 modified NFO-PMMA films (composite) are shown in Fig. 4(a, b). It is observed that the composites with modified NFO nanoparticles are almost uniformly distributed throughout the matrix, with small patches which are trying to pull up from the vicinity, which refers the reinforcement nature of silica [41-42]. On the other hand, the unmodified NFO-PMMA composite shows

patches but not pronounced which signifies lesser reinforcement due to the crystalline behaviour of NFO. However, the presence of SiO_2 groups adsorbed onto the NFO particles and enhanced the compatibility of the matrix. Hence, the interfacial interaction between modified nanoparticles and polymer matrix are stronger than that of the composite filled with pure NFO nanoparticles [42-43]. As a result, the dielectric and electrical performance of SiO_2 modified NFO-PMMA composites are also improved.

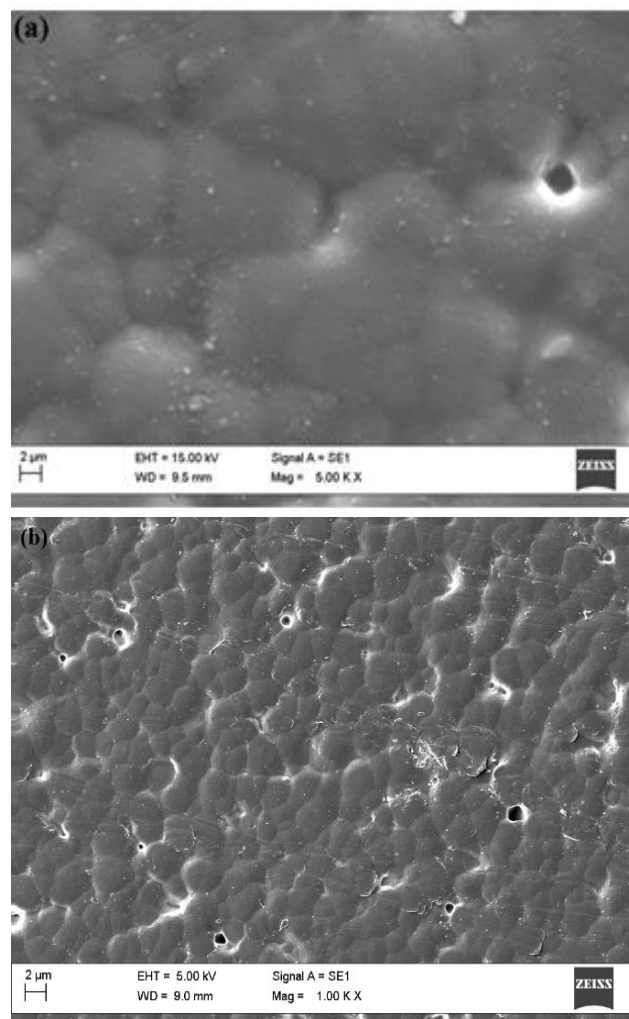


Fig. 4. SEM image of (a) NFO-PMMA and (b) SiO_2 @NFO-PMMA composite films.

Dielectric and electrical properties of NFO-PMMA composite films

Fig. 5 shows the frequency dependent dielectric constant (ϵ_r) of the NFO-PMMA and SiO_2 modified NFO-PMMA composite films with various weight percentage of NFO (contents) at room temperature. It is revealed that the dielectric constant increases with the increase of unmodified and modified NFO particles and decreases with increase in frequency over the entire frequency range. The value of ϵ_r decrease with increase in frequency (at low frequency region) can be explained on the basis of the

dispersion of the polarization. At lower frequency region, the dielectric constant of the composites is mainly contributed to the Maxwell-Wagner-Sillars (MWS) or interfacial polarization [44-45]. Moreover, the SiO₂ modified NFO-PMMA composites (NFO content is about 10wt %), the dielectric constant is ≈ 67 at 100 Hz, nearly 13 and 1 times higher than that of the pure PMMA and unmodified one (its dielectric constant is about 47 and 5 at 100 Hz). The modification of SiO₂ groups on NFO nanoparticles has improved the dispersion of particles in composites and the compatibility with the polymer matrix. Thus, the modified composite shows a good mixing with defect free such as agglomeration and/or cracks and leads to enhance the dielectric and electrical performance.

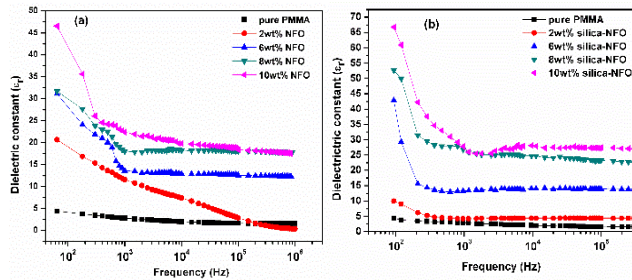


Fig. 5. Frequency dependence of dielectric constant of (a) NFO-PMMA and (b) SiO₂ modified NFO-PMMA composite films at room temperature.

Fig. 6 shows the dielectric loss (tanδ) with frequency for NFO-PMMA and SiO₂ modified NFO-PMMA composite films with various weight percentage of NFO in 100 Hz to 1 MHz frequency ranges at room temperature. It is seen that the value of tan δ increases gradually with increase in filler content over the whole frequency range. Meanwhile, the loss of the modified NFO-PMMA composites remain quite lower (< 0.5) than that of the unmodified one, which is mainly due to the surface modifiers between the interfaces of NFO and PMMA matrix with a positive impact on the interfacial polarization [46]. The SiO₂ modified NFO-PMMA composite films exhibit a high value dielectric constant (≈ 67) and reasonably low dielectric loss (≈ 0.35) at low frequency region (<1000 Hz), which is mainly the requirement of a composite material for energy storage devices.

To understand the mechanisms of dielectric properties for NFO-PMMA composites, the classic percolation theory is used to predict the dielectric constant of the SiO₂@NFO-PMMA composite for 100 Hz at room temperature. The variation of dielectric constant in the proximity of the percolation threshold power law, which is expressed as follows [47]:

$$\varepsilon = \varepsilon_1 (fc - f)^{-s} \quad \text{for } f < fc \quad (1)$$

where ε and ε_1 represent the dielectric constant of the composite and the PMMA matrix, respectively, f is the weight percentage of the SiO₂@NFO, fc is the percolation threshold and s is the critical exponent.

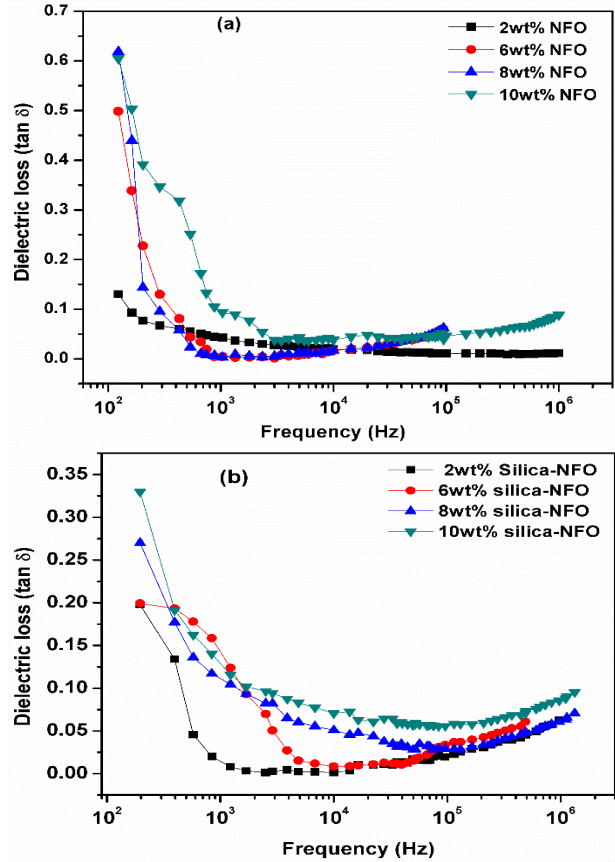


Fig. 6. Dielectric loss of the (a) NFO-PMMA and (b) SiO₂@NFO-PMMA composites with a different weight percentage of NFO contents as a function of frequency at room temperature.

The experimental results fit well (as shown in Fig. 7) with the dielectric constant to Equation (1) at percolation theory when the weight percentage of the modified NFO is less than 10 wt% (the fitting parameters $fc = 6wt\%$ and critical exponent $S = 0.976$, respectively). The linear fit of the double log-log value of ε_r (Equation-1) and the percentage (weight) of modified filler also indicates that the dielectric property of the composites fits well with percolation theory.

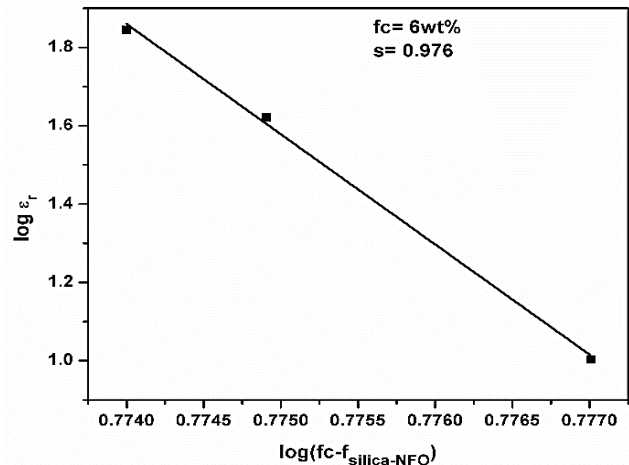


Fig. 7. Shows the best fits of the dielectric constant to Equation (1).

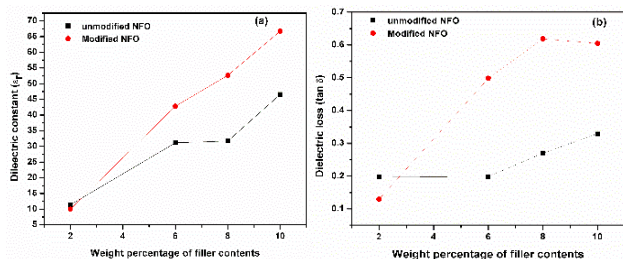


Fig. 8. Comparison of room temperature dielectric constant and dielectric loss of the NFO-PMMA and SiO₂@NFO-PMMA composites with a different weight percentage of NFO contents at 100 Hz.

Fig. 8 illustrates the dielectric properties of NFO-PMMA and SiO₂ modified NFO-PMMA composite films with a different weight percentage of NFO nanoparticles at 100 Hz. As shown in **Fig. 8**, it is clear that the value of ϵ_r as well as $\tan\delta$ increases gradually with the increase of NFO content. The dielectric properties of the composites is strongly influenced by surface morphology of ferrite particles, interface areas, agglomeration, increasing air voids and the large difference of ϵ_r between the ferrite particles and polymer matrix [48-50]. These aspects have negative influence on the dielectric properties of the unmodified NFO-PMMA composites and yields reduction in the dielectric constant. However, in the SiO₂ modified NFO-PMMA composites (**Fig. 8(a)**), the value of ϵ_r is higher than that of the unmodified NFO nanoparticles. This can be attributed to the presence of SiO₂ groups adsorbed on the NFO nanoparticles within the polymer matrix, which acts as a passive layer. This may be explained on the presence of SiO₂ layer around NFO nanoparticles with electron affinities (high). This can help to make strong dipole interaction between the functional groups of ferrite nanoparticles and polymer to get better distribution in the polymer matrix and create positive influences on the interfacial polarization [51-52]. On the other hand, loss tangent is another crucial parameter for the capacitor applications. As shown in **Fig. 7 (b)**, dielectric loss of composites increases gradually with the increase of filler contents (**Fig. 8(b)**) at 100 Hz. Besides, it is also noted the dielectric loss of all the composites still maintains at a relatively low level. For instance, the dielectric loss of 10 wt% of SiO₂@NFO-PMMA composite film is 0.025 at 100 Hz, which may be attributed to the factors which includes fewer defects at the interfaces and homogeneous dispersion of SiO₂ modified NFO particles in the PMMA matrix [53-54].

AC electrical conductivity study

Fig. 9 shows alternating current (AC) conductivity with frequency of unmodified and SiO₂ modified composites with various weight percentage of NFO. The ac conductivity of the composite increases with increase in frequency for different weight percentage of NFO and have little higher value than that of the pure PMMA over the whole frequency region. For the composites with modified NFO contents, the conductivity exhibits nearly frequency independent ($<10^3$ Hz) and signifies as dc

conductivity. However, the conductivity of the composite shows a dispersive behaviour in the higher frequency region, which increases linearly with increase in frequency and is signified as ac conductivity. When $f_{\text{SiO}_2@\text{NFO}}$ approaches f_c , the percolation threshold power law [55] is described as follows:

$$\sigma \propto \omega^\mu, \text{ as } f_{\text{SiO}_2@\text{NFO}} \rightarrow f_c \quad (2)$$

Here, $\omega=2\pi\nu$, where ν and μ are the frequency and corresponding critical exponent, respectively. The experimental data of the composite with $f_{\text{SiO}_2@\text{NFO}} = 6\text{wt}\%$ (near f_c) gives $\mu=0.97$ [**Fig. 9(b)**], which is a little higher than that of the normal value (0.7) obtained from the percolation theory [55].

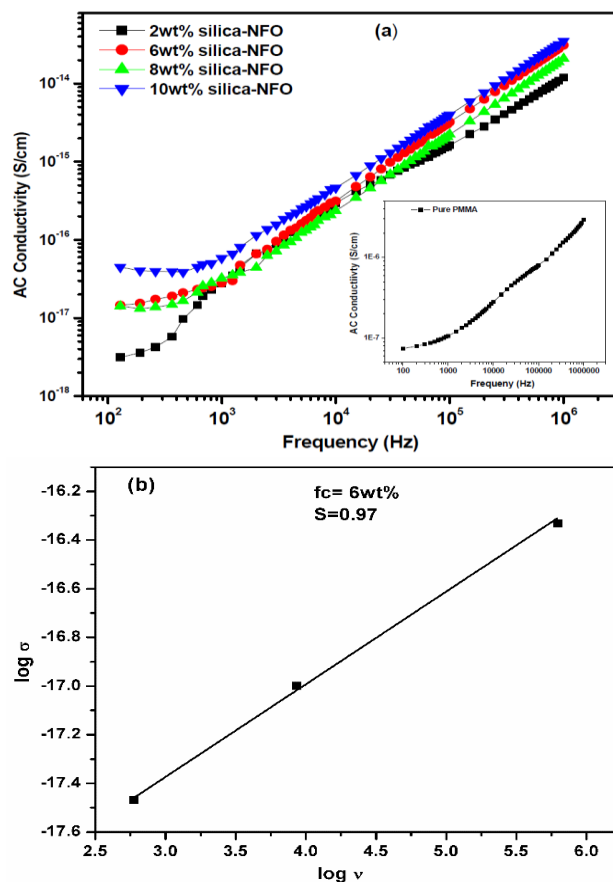


Fig. 9. Frequency dependence of AC conductivity of the (a) SiO₂@NFO-PMMA composites with a different weight percentage of NFO and (b) shows the best Fit of the AC conductivity of the composites with 6 wt% of SiO₂@NFO to Equation (2).

Conclusions

In summary, the SiO₂ modified NFO filled PMMA composite films were prepared through solution casting technique. XRD study confirmed the formation of the composites with fcc structure. FTIR spectra confirmed the presence of SiO₂ groups on the NFO nanoparticles, which could be improved the compatibility between the nanoparticles and the polymer matrix and also make the homogeneous dispersion of the composite films. Moreover, the SiO₂ modified composite exhibited high

dielectric constant (≈ 67) and relatively low dielectric loss (< 0.5) at 100 Hz. The dielectric constant followed the percolation scaling law with percolation threshold of $f_c=6$ wt% and the critical exponent of $s = 0.97$. These composites with the performance of high dielectric constant might be potential candidates for high energy storage devices.

Acknowledgements

The authors acknowledge the financial support through DRS-1 of UGC, New Delhi, India under SAP and FIST programme of DST, New Delhi, India for the development of research work in the School of Physics, Sambalpur University. One of the authors SM acknowledges the financial support of UGC through UGC-BSR fellowship scheme. One of the authors BB acknowledges to the SERB under DST Fast Track Scheme for Young Scientist (Project No. SE/FTP/PS-036/2011), New Delhi, India., and RNM acknowledges project grant of DST Govt. of Odisha, India.

Keywords

Poly (Methylmethacrylate), NiFe₂O₄, surface modification, dielectric properties, composites.

Received: 09 September 2019

Revised: 09 December 2019

Accepted: 23 December 2019

References

- Chao, F.; Liang, G.; Kong, W.; Zhang, X.; *Mater. Chem. Phys.*; **2008**, *108*, 306.
- Fan, B.H.; Zha, J.W.; Wang, D.R.; Zhao, J.; Zhang, Z.F.; Dang, Z.M.; *Compos. Sci. Technol.*; **2013**, *80*, 66.
- Kanna, R.R.; Lenin, N.; Sakthipandi, K.; Kumar, A.S.; *J. Magn. Magn. Mater.*; **2018**, *453*, 78.
- Liu, X.F.; Xiong, C.X.; Sun, H.J.; Dong, L.J.; Li, R.; Liu, Y.; *Mater. Sci. Eng. B*; **2006**, *127*, 261.
- Cheng, K.C.; Lin, C.M.; Wang, S.F.; Lin, S.T.; Yang, C.F.; *Mater. Lett.*; **2007**, *61*, 757.
- Rana, D.K.; Singh, S.K.; Kundu, S.K.; Roy, S.; Angappane, S.; Basu, S.; *New J. Chem.*; **2019**, *43*, 3128.
- Baruwati, B.; Reddy, K.; Manorama, S.; Singh, R.; Parkash, O.; *Appl. Phys. Lett.*; **2004**, *85*, 28333.
- Zhao, G.; Xu, J.J.; Chen, H.Y.; *Electrochem. Commun.*; **2006**, *8*, 148.
- Afshar, S.R.S.; Hasheminiasari, M.; Masoudpanah, S.M.; *J. Magn. Magn. Mater.*; **2018**, *466*, 1.
- Ma, J.; Hu, J.; Li, Z.; Nan, C.W.; *Adv. Mater.*; **2011**, *23*, 1062.
- Chu, X.; Jiang, D.; Zheng, C.; *Sens. Actuators B Chem.*; **2007**, *123*, 793.
- Rana, S.; Srivastava, R.S.; Sorensson, M.M.; Misra, R.D.K.; *Mater. Sci. Eng. B*; **2005**, *119*, 144.
- Raikher, Y.L.; Stepanov, V.I.; Depeyrot, J.; Sousa, M.H.; Tourinho, F.A.; Hasmonay, E.; *J. Appl. Phys.*; **2004**, *96*, 5226.
- Mishra, M.K.; Moharana, S.; Behera, B.; Mahaling, R.N.; *Front. Mater. Sci.*; **2017**, *11*, 82.
- Vaishnava, P.P.; Senaratne, U.; Buc, E.; Naik, R.; Naik, V.M.; Tsoi, V.G.; Wenger, L.E.; Boolchand, P.; *J. Appl. Phys.*; **2006**, *99*, 2165922.
- Sindhu, S.; Jegadesan, S.; Parthiban, A.; Vaiyaveetil, S.; *J. Magn. Magn. Mater.*; **2006**, *296*, 104.
- Chi, Q.; Ma, T.; Dong, J.; Cui, Y.; Zhang, C.; Xu, S.; Wang, X.; Lei, Q.; *Sci. Rep.*; **2017**, *7*, 3072.
- Boon, M.S.; Saw W.P.S.; Mariatti, M.; *J. Magn. Magn. Mater.*; **2012**, *324*, 755.
- Singh, K.; Ohlana, A.; Kotnala, R.K.; Bakhshi, A.K.; Dhawan, S.K.; *Mater. Chem. Phys.*; **2008**, *112*, 651.
- Wilson, J. L.; Poddar, P.; Frey, N. A.; Srikanth, H.; *J. Appl. Phys.*; **2004**, *95*, 1439.
- Testa, A.M.; Foglia, S.; Suber, L.; Fiorani, D.; Casas, L.; Roig, A.; Molins, E.; Greneche, J. M.; Tejada, J.; *J. Appl. Phys.*; **2001**, *90*, 1534.
- Dang, Z.M.; Yu, Y.F.; Xu, H.P.; J. Bai, J.; *Compos. Sci. Technol.*; **2008**, *68*, 171.
- Ramajo, L.; Castro, M.S.; Reboredo, M.M.; *Compos. Part A-Appl. S.*; **2007**, *38*, 1852.
- Taghvaei, A.H.; Shokrollahi, H.; Ebrahimi, A.; Janghorban, K.; *Mater Chem. Phys.*; **2009**, *116*, 247.
- Yan, W.; Han, Z. J.; Phung, B.T.; Ostrikov, K.; *ACS Appl. Mater. Interfaces*; **2012**, *4*, 2637.
- Luo, H.; Zhang, D.; Jiang, C.; Yuan, X.; Chen, C.; Zhou, K.; *ACS Appl. Mater. Interfaces*; **2015**, *7*, 8061.
- Xie, L.Y.; Huang, X.Y.; C. Wu, C.; Jiang, P.K.; *J. Mater. Chem.*; **2011**, *21*, 5897.
- Pascariu, P.; Airinei, A.; Asandulesa, M.; Rotaru, A.; *Polym. Int.*; **2018**, *67*, 1313.
- Nagarajan, K.; Muthusamy, A.; Chitra, P.; Anand, S.; Jayaprakash, R.; *J. Magn. Magn. Mater.*; **2017**, *423*, 208.
- Wang, R.; Xie, C.; Luo, S.; Gou, B.; Xu, H.; Zeng, L.; *RSC Adv.*; **2019**, *9*, 19648.
- He, F.; Lam, K.; Ma, D.; Fan, J.; Chan, L. H.; Zhang, L.; *Carbon*; **2013**, *58*, 175-84.
- Plyushch, A.; Macutkevi, J.; Banys, J.; Kuzhir, P.; Kalanda, N.; Petrov, A.; Clara Silvestre, C.; Uimin, M.A.; Yermakov, A.Y.; Shenderova, O.; *Coatings*; **2018**, *8*, 165.
- Martins, P.; Costa, C.M.; Botelho, G.; Lanceros-Mendez, S.; Barandiaranc, J.M.; Gutierrez, J.; *Mater. Chem. Phys.*; **2012**, *131*, 698.
- Menelaou, M.; Georgoula, K.; Simeonidis, K.; Samara, C.D.; *Dalton Trans.*; **2014**, *43*, 3626.
- Iqbal, Y.; Bae, H.; Rhee, I.; Hong, S.; *J. Magn. Magn. Mater.*; **2016**, *409*, 80.
- Ding, H. L.; Zhang, Y.X.; Wang, S.; Xu, J. M.; S. C. Xu, S.C.; Li, G.H.; *Chem. Mater.*; **2012**, *24*, 4572.
- Kim, K.D.; Kim, S.S.; Choa, Y.H.; Kim, H.T.; *J. Ind. Eng. Chem.*; **2007**, *13*, 1137.
- Reyes-Acosta, M.A.; Torres-Huerta, A. M.; Domínguez-Crespo, M. A.; Flores-Vela, A.I.; Dorantes-Rosales, H. J.; Ramírez-Meneses, E.; *J. Alloys Compd.*; **2015**, *643*, S150.
- Hashem, M.; Rez, M. F. A.; Fouad, H.; Elsarnagawy, T.; Elsharawy, M.A.; Umar, A.; Assery, M.; Ansari, S.G.; *Sci. Adv. Mater.*; **2017**, *9*, 938.
- Khairy, M.; Gouda, M.E.; *J. Adv. Res.*; **2015**, *6*, 555.
- Rattanasom, N.; Saowapark, T.; Deprasertkul, C.; *Polym. Test*; **2007**, *26*, 369.
- Xu, T.; Jia, Z.; Luo, Y.; Jia, D.; Peng, Z.; Xu, T.; Jia, Z.; Luo, Y.; Jia, D.; Peng, Z.; *Appl. Surf. Sci.*; **2015**, *328*, 306.
- Kuang, X.; Liu, Z.; Zhu, H.; *J. Appl. Polym. Sci.*; **2013**, *129*, 3411.
- Zhou, W.Y.; Wang, Z.J.; Dong, L.N.; Sui, X.Z.; Chen, Q.G.; *Compos Part A Appl. Sci. Manuf.*; **2015**, *79*, 183.
- Maji, P.; Choudhary, R.B.; Majhi, M.; *J. Non-Cryst. Solids*; **2017**, *456*, 40.
- Zhang, G.; Brannum, D.; Dong, D.; Tang, L.; Allahyarov, E.; Tang, S.; Kodweis, K.; Lee, J.K.; Zhu, L.; *Chem. Mater.*; **2016**, *28*, 4646.
- Feng, Y.; Li, W.L.; Wang, J.P.; Yin, J.H.; Fei, W.D.; *J. Mater. Chem A*; **2015**, *3*, 20313.
- Tomer, V.; Manias, E.; Randall, C.A.; *J. Appl. Phys.*; **2011**, *110*, 044170.
- Roy, M.; Nelson, J. K.; MacCrone, R. K.; Schadler, L.S.; Reed, C.W.; Keefe, R.; *IEEE Trans. Dielectr. Electr. Insul.*; **2005**, *12*, 629.
- Yu, K.; Niu, Y.; Zhou, Y.; Bai, Y.; Wang, H.; *J. Am. Ceram. Soc.*; **2013**, *96*, 2519.
- Tang, H.; Ma, Z.; Zhong, J.; Yang, J.; Zhao, R.; Liu, X.; *Colloids and Surfaces A: Physicochem. Eng. Aspects*; **2011**, *384*, 311.
- Niu, Y.; Bai, Y.; Yu, K.; Wang, Y.; Xiang, F.; Wang, H.; *ACS Appl. Mater. Interfaces*; **2015**, *7*, 24168.
- Calame, J. P.; *J. Appl. Phys.*; **2006**, *99*, 084101.
- Fu, J.; Hou, Y.; Zheng, M.; Wei, Q.; Zhu, M.; Yan, H.; *ACS Appl. Mater. Interfaces*; **2015**, *7*, 24480.
- Nan, C.W.; *Prog. Mater. Sci.*; **1993**, *37*, 1.